ACS APPLIED MATERIALS & INTERFACES

Research Article

www.acsami.org

Bio-Inspired Anti-Oil-Fouling Chitosan-Coated Mesh for Oil/Water Separation Suitable for Broad pH Range and Hyper-Saline Environments

Shiyan Zhang,[†] Fei Lu,[†] Lei Tao, Na Liu, Changrui Gao, Lin Feng,* and Yen Wei

Department of Chemistry, Tsinghua University, Beijing 100084, People's Republic of China

Supporting Information

ABSTRACT: Here, we report a bio-inspired chitosan (CS)-based mesh with high separation efficiency, oil-fouling repellency, and stability in a complex liquid environment. The surface of the CS coating maintains underwater superoleophobicity and low oil adhesion (<1 μN) in pure water and hyper-saline solutions, and it can keep stable special wettability in broad pH range environments after the CS mesh is fully cross-linked with glutaraldehyde and then reduced by sodium borohydride to form a stable carbon−nitrogen single bond. The separation process is solely gravity-driven, and the mesh can separate a range of different oil/water mixtures with >99% separation efficiency in hyper-saline and broad pH range conditions. We envision that such a separation method will be useful in oil spill cleanup and industrial oily wastewater treatment in extreme environments.

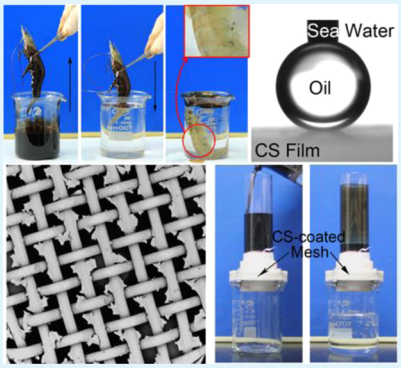

KEYWORDS: *underwater superoleophobic, oil/water separation, chitosan, broad pH range, hyper-saline, bio-inspired*

INTRODUCTION

Due to increasing industrial oily wastewater production as well as frequent oil spill accidents,[1−3] it is of great importance to create novel technologies to separate oil and water.[4−6] Conventional methods, such as skimming, gravity processing, ultrasonic separation, air flotation, membrane filtration, electrocoalescence, and biological treatment, suffer from limitations such as low separation efficiency, highly energy-consuming, generation of secondary pollutants, and high costs.[7−9] Therefore, it is highly desired to develop novel functional materials in the field of oil/water separation that are separation efficient, energy-efficient, environmentally friendly, resistant to oil fouling, cheap, and can maintain stable separation abilities even in complex practical environments.[10−12]

The interfacial energy difference of oil and water provides us with an idea to design high-efficiency oil/water separation materials.[13−16] Some hydrophobic/oleophilic materials,[17−19] so-called "oil-removing" materials, which can allow the permeation of oil, have aroused much interest.[20−23] However, they suffered from limitations such as being easily fouled by oil or being blocked up due to the intrinsic oleophilicity and being unsuitable for gravity-driven oil/water separation due to the higher density of water over most oil. Recently, we reported a novel "water-removing" type of separation material, which can realize both superhydrophilic and underwater superoleophobic properties simultaneously, by introducing a third repulsive water phase.[24] These materials can selectively filtrate or absorb water from oil with a high separation capacity, solely driven by gravity and resistance to oil fouling.[24−26] However, they are commonly sensitive to salt, acid, or alkaline in solution and can only be used under mild conditions.

Usually, oily wastewater is in complex acidic, alkaline, or hyper-saline conditions.[27,28] Thus, it is a challenge to create advanced materials with stable special wettability to separate oil and water in complex environments.[29−31] Nature, however, offers us excellent inspiration for the choice of materials. Shrimp shells have an anti-oil-fouling behavior in the ocean (with a saline environment), owing to the underwater superoleophobicity of the surface caused by its hydrophilic chemical composition. Inspired by this observation, we developed a novel bio-inspired functional material by coating chitosan (CS) on rough Cu mesh. The surface of the CS coating mesh is hydrophilic in air and superoleophobic in water, which can allow it to achieve rapid gravity-driven oil/water separation, even crude oil/water separation, with >99% efficiency both in pure water and hyper-saline solution. Furthermore, after modifying the CS coating by fully cross-linking, reduction, and adding polyvinyl alcohol (PVA), a stable CS/PVA coated mesh for oil/water separation suitable for a broad pH range (pH 1−13) and hyper-saline solutions is obtained. To the best of our knowledge, this is the first example that gravity-driven oil/water separation can be realized in a broad pH range and hyper-saline environments, which is important with respect to the potential use for oily wastewater treatment even in complex environments.

Received: September 2, 2013
Accepted: November 1, 2013
Published: November 1, 2013

dx.doi.org/10.1021/am403203q | ACS Appl. Mater. Interfaces 2013, 5, 11971−11976

EXPERIMENTAL SECTION

Fabrication of CS Film. CS solutions were prepared by dispersing 2 g of CS (degree of deacetylation = 80.0%−95.0%, viscosity = 50−800 mPa s) into 100 mL of acetic acid solution (2 wt %) while stirring on a magnetic stirrer plate for over 24 h. As for the slightly cross-linked CS, the 1 wt % glutaraldehyde (GA) solution (0−3.70 mL) was added to the 100 mL CS solution before degassing on a stand. After that, the solution was dripped on a clean glass plate while the glass plate was placed on a spin coater, spinning with a speed of 400 r/min for 9 s and later at 1000 r/min for 30 s to better spread the solution uniformly on the plate. Then, the plate attached with CS film was immersed in NaOH solution (4 wt %) for 1 min and washed with deionized water. The preservation environment was deionized water or salt solution, depending on the test environment. All experiments were conducted at room temperature. Seawater (3.5 wt %) was obtained by mixing deionized water and seacrystal (the remains of seawater after evaporation, purchased from Fish market, Tsinghua University, Beijing).

Electrodeposition of the Cu Substrate. Phosphor copper meshes (300 mesh size) were selected as the substrate material. The meshes were immersed in a solution of HCl(aq) (3.7 wt %) for 1 h to remove the CuO on the surface. After that, the meshes were rinsed with deionized water rapidly. Then, Cu electrodeposition was carried out on these surfaces at a constant potential (1.5 V) for 1 min at room temperature in a stationary electrolyte without stirring or air bubbling, where the electrolyte was a solution of $CuSO_4$(aq) (16 wt %). Both the working electrode and cathode were clean Cu mesh. After the deposition, the samples were rinsed with deionized water and dried with compressed air.

Fabrication of CS-Coated Mesh. The rough copper mesh was carefully immersed in the CS/GA (100 mL CS solution added with 3.70 mL of GA solution (1 wt %)) mixed acetic acid solution for 5 min and then drawn out slowly with the solution adhered on the surface of the copper wires. After the mesh was dried in air, it was immersed in NaOH (4 wt %) solution for 1 min and washed with deionized water. Then, the CS-coated mesh was acquired and was later preserved in deionized water or NaCl solution (2 mol L^{-1}). The modification method was as follows: PVA was dissolved in deionized water at 90 °C with a concentration of 10 wt %. The PVA solution was then mixed with CS solution [CS (2 wt %)/PVA (10 wt %) = 4:1 (v:v)], stirring together for 1 h to form a homogeneous solution. The rough copper mesh was immersed in the mixture solution for 5 min, drawn out, dried in the air, and washed with NaOH (4 wt %) and deionized water. Then, the CS/PVA coated mesh was immersed in GA solution (1 wt %) at 40 °C for 30 min to be fully cross-linked and later was immersed in a reducing solution (mixed solution containing 1.5 wt % $NaBH_4$ and 1 wt % NaOH) at 40 °C for 30 min. After it was washed with deionized water and dried in air, the CS/PVA coated mesh was obtained.

Characterization. Scanning electronic microscope (SEM) images of the substrates were obtained using a field-emission scanning electron microscope (Phenom G2 pure desktop SEM). Atomic force microscope (AFM) images were acquired using a scanning probe microscope (SEIKO SPI3800N/SPA400, Tokyo, Japan). Contact angles were measured on an OCA20 machine (Data-Physics) at ambient temperature. Considering the underwater test, the oil droplets (1,2-dichloroethane (DCE), about 2 μL) were dropped carefully onto the materials, which were immersed in water. The average value of five measurements performed at different positions on the same sample was adopted as the contact angle. The oil-adhesion forces were measured using a high-sensitivity microelectromechanical balance system (Data-Physics DCAT 11) underwater. An oil droplet (1,2-dichloroethane (DCE), 5 μL) was suspended with a metal cap was controlled to contact the surface to the CS film surface at a constant speed of 0.005 mm s^{-1} and then removed. The forces were recorded during the whole time, the adhesive force was defined as the force required to take the oil drop away from the substrate.

Oil/Water Separation. The as-prepared mesh was fixed between two Teflon fixtures. The diameter of the tube was 30 mm. The oil/water mixtures (30% v/v, stirred before separation) were poured onto the as-prepared mesh. The separation was achieved by the gravity of the liquids. After separation, we waited for at least 1 min before taking away the collected water. The oil concentration of the collected water after separation was measured by the infrared spectrometer oil content analyzer (CY2000, China). CCl4 was used to extract oils from water. Then, the absorbance at 2930, 2960, and 3030 cm^{-1} was measured. Through calculation with the absorbance and the correction coefficient, the oil content can be obtained. The separation efficiency (R (%)) is calculated according to eq 1:

$$R\ (\%) = \left(1 - \frac{C_P}{C_0}\right) \times 100\% \quad (1)$$

where C_0 and C_p are the oil content of the oil/water mixture before and after separation.

RESULTS AND DISCUSSION

Shrimp Shell. Figure 1 shows the anti-oil-fouling behavior of a shrimp shell in seawater. The shrimp shell, even stained by

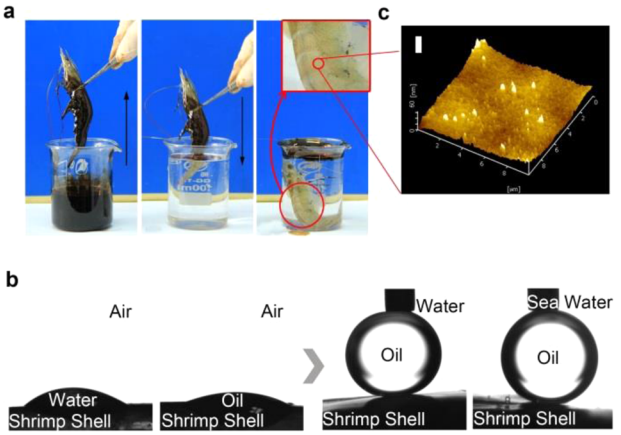

Figure 1. Underwater anti-oil-fouling behavior of shrimp shell. (a) The sequences of images indicate that both shrimp shell, stained by crude oil, can clean itself after placed in seawater. (b) The wettability of the CS film, showing hydrophilic and oleophilic properties, but superoleophobic in both deionized water and seawater. The statistic contact angle was measured when the droplet was stable on the surface. (c) An AFM image of the shrimp shell (scale bar is 60 nm).

crude oil, can clean itself thoroughly when placed in seawater (Figure 1a). We also characterized the wetting behavior of water and oil on the surface of the shrimp shell both in air and under water. The contact angle (CA) measurement shows that the shrimp shell is hydrophilic and oleophilic in air, with static CAs of 41.1 ± 3.6° (2 μL, deionized water) and 24.7 ± 5.5° (2 μL, 1,2-dichloroethane (DCE)), respectively. However, when the shrimp shell is placed in deionized water and seawater, it exhibits an underwater superoleophobic property with static oil CAs over 150° (Figure 1b). The underwater oil-adhesion force measurement showed that the shrimp shell can keep an oil-adhesion force smaller than 1 μN in both deionized water and seawater (see Supporting Information, Figure S1a). These results indicate the shrimp shells can maintain stable superoleophobic and low oil-adhesion properties that are not influenced by the salt dissolved in water. Such special wettability is believed to be the main reason for its oil-fouling-resistant behavior in more complicated marine environments with hyper-saline concentrations.

As reported, the special wettability is governed by both the surface microstructures and the surface chemical composi-

tion.[32,33] Therefore, we first investigated the surface microstructures of the shrimp shell using both an atomic force microscope (AFM) and a scanning electronic microscope (SEM). The AFM (Figure 1c) and SEM images (see Supporting Information, Figure S2a) show that the shrimp shell surface is flat on a microscale, while having random nanostructures with an average root-mean-squared (RMS) roughness of 8 nm. The result indicates that in this solid/liquid/liquid system, the chemical composition of a shrimp shell may play a more important role for the special wettability. This result may due to the hydrophilicity of the shrimp shell surface. With this hydrophilicity, water can be trapped on its surface, forming a layer of water on its surface and blocking up the oil. It is expected that we can artificially fabricate the bio-inspired film with an anti-oil-fouling property using the hydrophilic material with a surface chemical composition similar to that of the shrimp shell.

CS Film. Chitin is a main composite of shrimp shells, but it is difficult to dissolve and does not form films.[34] Therefore, we select chitosan (CS), the deacetylation form of chitin, which can dissolve in an acid solution to fabricate a bio-inspired film. CS is a hydrophilic polymer with many hydroxyl and amino groups. In addition, CS is an ideal, inexpensive coating material with properties of nontoxicity and biocompatibility.[35,36] The CS films are obtained by spin coating of a CS acetic acid solution on glass slides at ambient atmospheric temperature (Figure 2a). We took two series of time-sequence optical images to compare the underwater self-cleaning capacity of the original glass slide and the CS-coated glass slide when both of them were stained by crude oil. The crude oil was stained on the surface of the original glass slide but can be cleaned thoroughly on the surface of the CS film (Figure 2b). This indicates that, compared with the surface of the original glass slide, the CS-coated slide shows a superior repellence to crude oil underwater. AFM (Figure 2c) and SEM images (see Supporting Information, Figure S2b) show that the bio-inspired CS film is flat on the microscale and has random nanostructures with an RMS roughness of 43 nm.

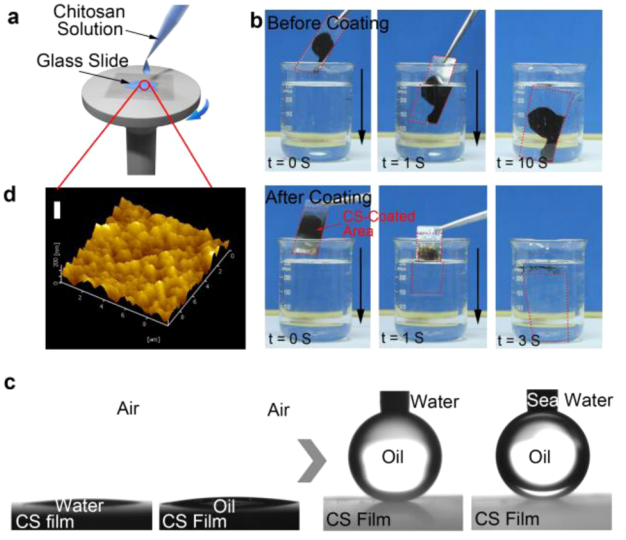

Figure 2. Fabrication of biomimetic chitosan film and its wettability characterization. (a) The schematic indicates film is obtained by spin coating the CS solution on a glass slide. (b) The sequence images compare self-cleaning (stained by crude oil) behavior of original glass slide and CS-coated one underwater. (c) An AFM image of the CS film (scale bar is 200 nm). (d) The wettability of the CS film, which is oleophilic and hydrophilic in air, whereas it is superoleophobic in deionized water and seawater.

The subsequent wettability characterization of the as-prepared CS film shows that the surface shares the special wettability behavior with shrimp shells (Figure 2d): the surface of CS film is hydrophilic (CA = 7.1 ± 3.0°) and oleophilic (CA = 11.8 ± 2.0°) in air whereas it possesses underwater superoleophobicity (2 μL, DCE, CA = 155.9 ± 1.0° in deionized water, CA = 153.0 ± 1.4° in seawater) and low oil-adhesion force in both pure water and seawater (<1 μN, see Supporting Information, Figure S1b).

CA characterization in sodium chloride (NaCl) solutions with different NaCl concentrations shows that the CS film surface can maintain its property of underwater superoleophobicity even in a saturated NaCl solution (Figure 3a).

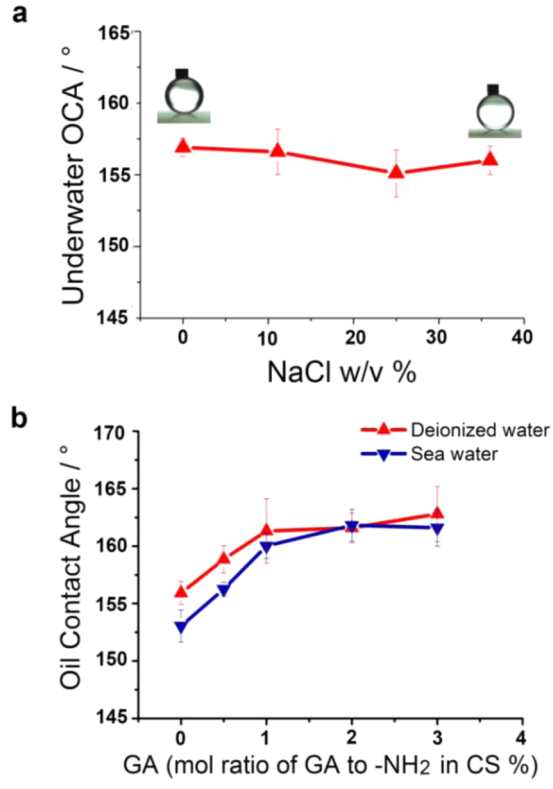

Figure 3. (a) The CS film can keep a stable underwater superoleophobic property even in saturated NaCl solution. (b) When slightly cross-linking the coating by adding glutaraldehyde (GA), the oil contact angles (OCAs) range from 155.9 ± 1.0° to 162.8 ± 2.4° in deionized water, whereas the OCAs range from 153.0 ± 1.4° to 161.6 ± 1.6° in seawater. Test was done within 4 h.

This result proves that the CS film has a stable underwater superoleophobicity and low oil-adhesion characteristics in a hyper-saline solution. In addition, the oleophobicity can be further enhanced by slightly cross-linking the CS using GA. With the increase of GA content from 0% to 2% (the mol ratio of GA to $-NH_2$ in CS) in the hybrid polymer network, the underwater OCAs increase from 155.9 ± 1.0° to 161.3 ± 2.8° on CS film surfaces and maintain a low oil-adhesion force of less than 1 μN at the same time, followed by a plateau when GA content increases from 2% to 3% (Figure 3b). Moreover, such a film can keep its stable underwater superoleophobicity

characteristics in both pure water and hyper-saline solution for at least 7 days (see Supporting Information, Table S1). Such a stable underwater superoleophobic surface has many potential applications in developing antifouling materials with high-efficiency oil/water separation.

CS-Coated Mesh. To achieve oil/water separation, CS-coated meshes were designed and prepared. Three hundred mesh-size Cu meshes (with an average porous diameter of approximately 50 μm) were chosen as the substrate for separation mesh. Previously, we studied the influence of microporosity and set up a model to calculate the theoretical intrusion pressure (P):[24]

$$P = 2\gamma_{L_1L_2}\cos\theta_0/d$$

where $\gamma_{L_1L_2}$, $\cos\theta_0$, and d are the water/oil interfacial tension, the oil contact angle on a flat surface, and the average diameter of the pore, respectively. However, when choosing a 400 mesh size (with average porous diameter of approximately 39 μm), we found that the pores were easily blocked up by chitosan (see Supporting Information, Figure S3). To find a balance between increasing the intrusion pressure and preventing blocking up, we chose to use the 300 mesh-size mesh as the substrate. The slightly cross-linked CS (cross-linked by GA with a content of 3% (the mol ratio of GA to $-NH_2$ in CS)), with a superior underwater superoleophobicity, was selected as the coating material by its glutaraldehyde (GA) content of 3% (the mol ratio of GA to $-NH_2$ in CS). Figure 4a shows the schematic illustration of the fabrication process of a CS-coated mesh. The fabrication generally consisted of two steps: electrodeposition and coating. Because there was no chemical bond between the substrate and coating, we cannot directly adhere the CS on the mesh. Thus, the electrodeposition of Cu on the Cu mesh, which can increase the contact surface, was designed to increase the adhesion between the coating and the mesh. Scanning electron microscope (SEM) images of the rough Cu mesh and CS-coated mesh are shown in Figure 4b,c, respectively. The rough Cu mesh is evenly covered with Cu grains (1−5 μm in diameter, Figure 4b). After the mesh was coated with CS, it is apparent that the rough Cu mesh was uniformly covered with CS film (Figure 4c).

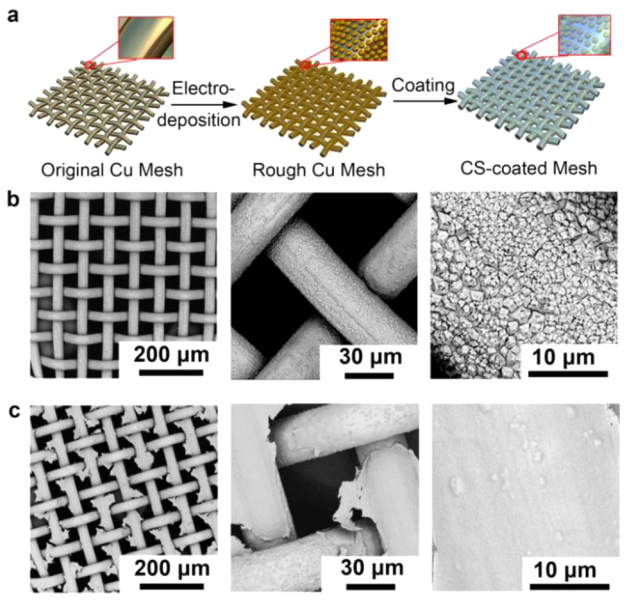

Figure 4. Design of CS-coated mesh. (a) The Schematic shows the fabrication process is mainly made up of two steps: first, enhancing the adhesion between coating and mesh by electrodepositing Cu on Cu mesh, and then coating the mesh by dipping it into the CS solution. The inserted images are details of meshes. (b) Different magnification SEM images show that rough Cu mesh, with an average pore diameter of about 50 μm, is covered with intensive Cu grains on its surface. (c) CS is uniformly coated on the surface of rough Cu mesh with random nano papillae.

The prepared CS-coated mesh can be used successfully to separate the mixtures of various oil and water with a separation efficiency higher than 99% (Figure 5b, yellow bar). The gravity-driven separation process of a crude oil and water mixture (30% v/v) was shown as an example (Figure 5a and the Supporting Information video). CS is a kind of hydrophilic polymer that is easy to form hydrogel,[35,36] thus, water can be trapped in the cross-linked network and forms a layer of water on its surface. When the water/oil mixture was poured onto the CS-coated mesh, such a layer of water between CS film and the mixture can result in the water passing freely while the oil blocks up. The saline mixture with oil and NaCl solution (2 mol L^{-1}) can also be successfully separated with >99% efficiency (Figure 5b, purple bar), indicating that the mesh can maintain a stable separation capacity in a hyper-saline environment. The chitosan-coated mesh is a promising functional material for oil spill cleanup in complex marine environments.

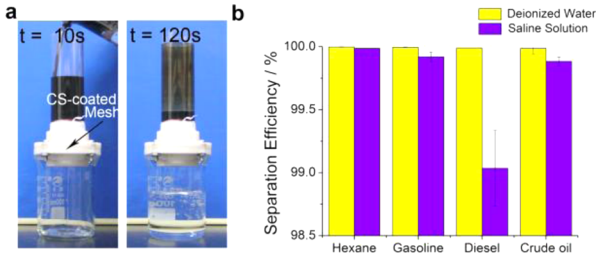

Figure 5. Assessment of oil/water separation ability of the CS-coated mesh. (a) The separation apparatus consists of the CS-coated mesh sandwiched between two fixtures made of Teflon into a filter: the top fixture was attached to a glass tube, whereas the bottom was placed on a beaker. The mixture of crude oil and water was poured into the glass tube. Water can pass through the mesh quickly whereas crude oil remains on the surface. The crude oil and water are separated thoroughly by the CS-coated mesh. (b) The separation efficiency of the CS-coated mesh shown for a series of oil mixed with deionized water and hyper-saline (2 mol L^{-1} NaCl solution).

Modified CS-Coated Mesh. Considering the industrial application, oil/water separation meshes are often needed to be used in acidic or alkaline environments. The as-prepared CS film can maintain stability in alkaline solution; however, it is very sensitive to acidic environments because the amino group is easily protonized in acidic solution. To solve this problem, the CS film should be completely cross-linked and reduced to protect the amino group. However, because the completely cross-linked CS films tend to be very brittle, polyvinyl alcohol (PVA) was added to maintain necessary toughness (Figure 6a). The modified CS film can realize the superoleophobicity with underwater OCAs above 150° from pH 1 to 13 (Figure 6b, yellow bar) and maintain this stable property for at least 7 days (see Supporting Information, Table S2). The ability of oil/water separation in acid, neutral, and alkali conditions was evaluated by testing the separation efficiency of a mixture of

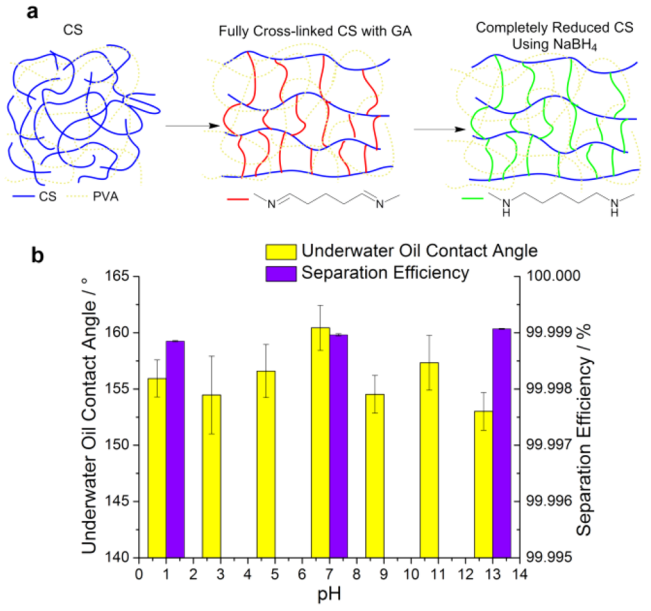

Figure 6. Modifying the CS-coating to maintain stable in broad pH range. (a) The CS coating was fully cross-linked and reduced to protect $-NH_2$ in acid condition. PVA was added to improve toughness. (b) The underwater wettability and oil/water separation efficiencies of the modified CS-coated mesh are shown. The OCAs (2 μL, DCE) of the modified CS-coated mesh are above 150°, and the separation efficiency are over 99.99% in broad pH range environments. The mixture of hexane and pH 1, pH 7, or pH 13 solutions was selected to do separation.

hexane and pH 1 solution, pH 7 solution, or pH 13 solution. The aqueous solution can pass through the mesh quickly whereas the oil is held at the mesh with separation efficiencies all above 99.99% (Figure 4b, purple bar, and see Supporting Information, Figure S4 and Table S3). More importantly, the mesh can be cleaned easily using water and can be reused over 30 times, due to its underwater anti-oil-fouling property (see Supporting Information, Table S4 and Figure S5). This modified CS-coated mesh can also separate other oil/water mixtures such as gasoline/water (see Supporting Information, Figure S6). This mesh, with excellent superoleophobicity in a broad pH range, has further potential applications in complex industrial oily wastewater treatment.

CONCLUSIONS

In summary, inspired by the anti-oil-fouling property of shrimp shells in the ocean, we fabricated a bio-inspired CS film with underwater superoleophobic and low oil-adhesive properties in water and in hyper-saline solutions. Then, a rough Cu mesh was used as a strong substrate to fabricate a CS-coated mesh. Owing to the stable special underwater wettability of the mesh surface, the mesh could realize an excellent gravity-driven oil/water separation capability, with oil-fouling resistance and reusability in both non-saline and hyper-saline conditions. Furthermore, we improved the stability under acidic conditions of the mesh through modifying the CS coating by fully cross-linking, reduction, and adding PVA, to meet the need of applications in acidic or alkaline conditions. This novel functional material has a wide range of application including the cleanup of marine oil spills, treatment of complicated industrial oily wastewater, and fuel purification.

ASSOCIATED CONTENT

Supporting Information

Photographs of the dynamic underwater oil-adhesion measurements on shrimp shell and CS film in seawater, SEM images of shrimp shell surface and CS film at different magnifications, SEM image of CS coated 400 mesh-size copper mesh, photographs of hexane/acid solution (pH = 1) separation and hexane/alkali solution (pH = 13) separation, SEM images of the modified CS-coated mesh before and after multiple (30 or 100) times of separation, separation efficiency graph, oil contact angles of the CS film in water and in 2 mol/L NaCl solution when tested at different times, oil contact angles of the modified-CS film in acidic and alkaline conditions when tested at different times, separation time and corresponding average flux and the oil/water separation test evaluated using a mixture of hexane and different solution, oil contact angles and separation efficiency of the modified CS-coated mesh in acidic and alkaline conditions after 30 separations, separation efficiency of the modified CS-coated mesh in saline/acidic and saline/alkaline conditions, and video of crude oil/water separation process of CS-coated mesh in hyper-saline condition. This material is available free of charge via the Internet at http://pubs.acs.org.

AUTHOR INFORMATION

Corresponding Author

*L. Feng. Tel: +86-10-6279-2698. E-mail: fl@mail.tsinghua.edu.cn.

Author Contributions

†S. Z. and F. L. contributed equally to this work.

Notes

The authors declare no competing financial interest.

ACKNOWLEDGMENTS

Authors acknowledge financial support from the National Natural Science Foundation (51173099), the National High Technology Research and Development Program of China (2012AA030306), and the National Research Fund for Fundamental Key Projects (2011CB935700).

REFERENCES

(1) Jernelov, A. *Nature* **2010**, *466*, 182−183.
(2) Gossen, L. P.; Velichkina, L. M. *Pet. Chem.* **2006**, *46*, 67−72.
(3) Srivastava, A.; Srivastava, O. N.; Talapatra, S.; Vajtai, R.; Ajayan, P. M. *Nat. Mater.* **2004**, *3*, 610−614.
(4) Adebajo, M. O.; Frost, R. L.; Kloprogge, J. T.; Carmody, O.; Kokot, S. *J. Porous Mater.* **2003**, *10*, 159−170.
(5) Nordvik, A. B.; Simmons, J. L.; Bitting, K. R.; Lewis, A.; StromKristiansen, T. *Spill Sci. Technol. Bull.* **1996**, *3*, 107−122.
(6) Shannon, M. A.; Bohn, P. W.; Elimelech, M.; Georgiadis, J. G.; Marinas, B. J.; Mayes, A. M. *Nature* **2008**, *452*, 301−310.
(7) McCloskey, B. D.; Ju, H.; Freeman, B. D. *Ind. Eng. Chem. Res.* **2010**, *49*, 366−373.
(8) Yoon, K.; Kim, K.; Wang, X.; Fang, D.; Hsiao, B. S.; Chu, B. *Polymer* **2006**, *47*, 2434−2441.
(9) Zhang, X.; Zhang, T.; Ng, J.; Sun, D. D. *Adv. Funct. Mater.* **2009**, *19*, 3731−3736.
(10) Tuteja, A.; Choi, W.; Ma, M.; Mabry, J. M.; Mazzella, S. A.; Rutledge, G. C.; McKinley, G. H.; Cohen, R. E. *Science* **2007**, *318*, 1618−1622.
(11) Yuan, J.; Liu, X.; Akbulut, O.; Hu, J.; Suib, S. L.; Kong, J.; Stellacci, F. *Nat. Nanotechnol.* **2008**, *3*, 332−336.
(12) Wang, C.; Yao, T.; Wu, J.; Ma, C.; Fan, Z.; Wang, Z.; Cheng, Y.; Lin, Q.; Yang, B. *ACS Appl. Mater. Interfaces* **2009**, *1*, 2613−2617.

(13) Srinivasan, S.; Chhatre, S. S.; Mabry, J. M.; Cohen, R. E.; McKinley, G. H. *Polymer* **2011**, *52*, 3209−3218.
(14) Kwon, G.; Kota, A. K.; Li, Y.; Sohani, A.; Mabry, J. M.; Tuteja, A. *Adv. Mater.* **2012**, *24*, 3666−3671.
(15) Peng, J.; Liu, Q.; Xu, Z.; Masliyah, J. *Adv. Funct. Mater.* **2012**, *22*, 1732−1740.
(16) Yang, J.; Zhang, Z.; Xu, X.; Zhu, X.; Men, X.; Zhou, X. *J. Mater. Chem.* **2012**, *22*, 2834−2837.
(17) Zhang, X. W.; Zhang, T.; Ng, J.; Sun, D. D. *Adv. Funct. Mater.* **2009**, *19*, 3731−3736.
(18) Huang, X. F.; Lim, T. T. *Desalination* **2006**, *190*, 295−307.
(19) Lee, C.; Baik, S. *Carbon* **2010**, *48*, 2192−2197.
(20) Feng, L.; Zhang, Z. Y.; Mai, Z. H.; Ma, Y. M.; Liu, B. Q.; Jiang, L.; Zhu, D. B. *Angew. Chem., Int. Ed.* **2004**, *43*, 2012−2014.
(21) Wang, L.; Yang, S.; Wang, J.; Wang, C.; Chen, L. *Mater. Lett.* **2011**, *65*, 869−872.
(22) Zhang, J.; Seeger, S. *Adv. Funct. Mater.* **2011**, *21*, 4699−4704.
(23) Wu, J.; Chen, J.; Qasim, K.; Xia, J.; Lei, W.; Wang, B. *J. Chem. Technol. Biotechnol.* **2012**, *87*, 427−430.
(24) Xue, Z.; Wang, S.; Lin, L.; Chen, L.; Liu, M.; Feng, L.; Jiang, L. *Adv. Mater.* **2011**, *23*, 4270−4273.
(25) Kota, A. K.; Kwon, G.; Choi, W.; Mabry, J. M.; Tuteja, A. *Nat. Commun.* **2012**, *3*, 1025−1025.
(26) Tian, D.; Zhang, X.; Tian, Y.; Wu, Y.; Wang, X.; Zhai, J.; Jiang, L. *J. Mater. Chem.* **2012**, *22*, 19652−19657.
(27) Kajitvichyanukul, P.; Hung, Y.-T.; Wang, L. K. *Membrane and Desalination Technologies; Handbook of Environment Engineering*; The Humana Press Inc.: Totowa, NJ, 2011; Vol. *13*, p 639.
(28) Kajitvichyanukul, P.; Hung, Y.-T.; Wang, L. K. *Advanced Physicochemical Treatment Processes; Handbook of Environment Engineering*; The Humana Press Inc.: Totowa, NJ, 2006; Vol. *4*, p 521.
(29) Feng, L.; Yang, Z.; Zhai, J.; Song, Y.; Lin, B.; Ma, Y.; Yang, Z.; Jiang, L.; Zhu, D. *Angew. Chem., Int. Ed.* **2003**, *42*, 4217−4220.
(30) Zimmermann, J.; Artus, G. R. J.; Seeger, S. *Appl. Surf. Sci.* **2007**, *253*, 5972−5979.
(31) Liu, M.; Xue, Z.; Liu, H.; Jiang, L. *Angew. Chem., Int. Ed.* **2012**, *51*, 8348−8351.
(32) Cassie, A. B. D.; Baxter, S. *Trans. Faraday Soc.* **1944**, *40*, 546−550.
(33) Feng, L.; Li, S. H.; Li, Y. S.; Li, H. J.; Zhang, L. J.; Zhai, J.; Song, Y. L.; Liu, B. Q.; Jiang, L.; Zhu, D. B. *Adv. Mater.* **2002**, *14*, 1857−1860.
(34) Ferrer, J.; Paez, G.; Marmol, Z.; Ramones, E.; Garcia, H.; Forster, C. F. *Bioresour. Technol.* **1996**, *57*, 55−66.
(35) Kumar, M. N. V. R. *React. Funct. Polym.* **2000**, *46*, 1−27.
(36) Rinaudo, M. *Prog. Polym. Sci.* **2006**, *31*, 603−632.